(Roche Diagnostics, Mannheim, Germany), chymotrypsin (Roche Diagnostics, Mannheim, Germany), or thermolysin at 37 °C for 6–20 h. The digests were extracted from the gel twice with 100 μl of 0.1% TFA containing 60% acetonitrile. These two extracts were combined, evaporated in a Speed-Vac, and stored at −80 °C until assayed.

Liquid chromatography-ion trap mass spectrometry (LC–MS/MS). The sample was resuspended in 0.1% formic acid containing 2% acetonitrile and applied to a Paradigm MS4 (Microm BioResources Inc., Auburn, CA) HPLC system fitted with HTC-PAL automatic sampler (CHROMSYS LLC, Alexandria, VA). A reverse-phase capillary column (Develosil ODS-HG5, 0.075 mm i.d. × 50 mm or 0.075 mm i.d. × 150 mm, Nomura Chemical Co., Ltd., Seto, Japan) was used at a flow rate of 200 or 300 nl/min with a 4–80% linear gradient of acetonitrile. Eluted peptides were directly detected with an ion trap mass spectrometer, LXQ (Thermo Fisher Scientific Inc.) at a spray voltage of 1.9 kV and collision energy of 35%. The

mass acquisition method consisted of one full MS survey scan followed by MS/MS scan of the most abundant precursor ions from the survey scan. Dynamic exclusion for MS/MS spectra was set to 30 s. Furthermore, if neutral loss of 98, 49, or 32.7 Da was detected (corresponding to loss of phosphoric acid from singly, doubly, and triply charged precursor ions) among the most abundant ions in the MS/MS scan, a MS/MS/MS scan was then carried out. The data were analyzed with BioWorks (Thermo Fisher Scientific Inc.) and Mascot (Matrix Science Inc., Boston, USA) software.

Calcium phosphate precipitation. Calcium phosphate precipitation was carried out as described [10]. Some extracted digests were dissolved in 44 μl of pure water, which was obtained from an EASYpure system (Barnstead International, Thermo Fisher Scientific Inc.). Then 2 μl of 0.5 M Na_2HPO_4 and 2 μl of 2 M NH_4OH were added and mixed, followed by the addition of 2 μl of 2 M $CaCl_2$. The solution was vortexed and centrifuged at 18,000g for 30 min. The supernatant was removed, and the precipitate was

Table 1
Identified phospho-peptides obtained from CK1 phosphorylated TDP-43.

Residue	Amino acid sequence	Charge	Mass (actual)	Mass (calculated)
Trypsin digestion				
83–95	RKMDETDASS(p)AVK	2	1516.87	1516.66
83–95	RKM(ox)DETDASS(p)AVK	2	1533.30	1532.65
84–95	KMDETDASS(p)AVK	1	1360.53	1360.65
84–95	KM(ox)DETDASS(p)AVK	2	1377.22	1376.55
85–95	MDETDASS(p)AVK	2	1233.40	1232.46
85–95	M(ox)DETDASS(p)AVK	2	1249.29	1248.46
85–95	M(ox)DETDAS(p)S(p)AVK	2	1329.16	1328.42
85–95	MDET(p)DASSAVK	2	1232.72	1232.46
85–97	MDETDASS(p)AVKVK	2	1461.46	1459.63
115–136	TT(p)EQDLKEYFSTFGEVLMVQVK	3	2688.66	2687.24
177–189	LPNSKQS(p)QDEPLR	2	1669.54	1670.71
182–189	QS(p)QDEPLR	2	1051.31	1051.43
228–251	AFAFVFTADDQIAQS(p)LCGEDLIIK	2	2694.69	2694.27
252–263	GIS(p)VHISNAEPK	2	1332.31	1330.63
269–275	QLERS(p)GR	2	925.98	924.42
276–293	FGGNPGGFGNQGGFGNS(p)R	2	1807.23	1805.73
409–414	SS(p)GWGM	1	703.22	703.20
409–414	S(p)S(p)GWGM(ox)	2	798.90	799.16
Chymotrypsin digestion				
1–27	MS(p)EY(p)IRVTEDENDEPIEIPSEDDGTVL	2	3254.58	3254.31
5–27	IRVTEDENDEPIEIPSEDDGT(p)VL	2	2664.68	2664.17
277–299	GGNPGGFGNQGGFGNS(p)RGGGAGLGNNQGSNMGGGMNF	2	2072.66	2070.87
386–401	GS(p)ASNAGSGSGFNGGF	2	1451.54	1452.53
386–401	GSAS(p)NAGSGS(p)GFNGGF	2	1533.92	1532.50
398–414	NGGFGSSMDS(p)KSSGWGM(ox)	2	1787.11	1786.63
Thermolysin digestion				
86–96	DETDASS(p)AVKV	2	1201.54	1200.49
236–249	DDQIAQS(p)LCGEDLI	2	1599.12	1598.65
242–250	S(p)LCGEDLII	1	1117.63	1117.44
270–276	LERS(p)GR	2	942.12	943.43
295–305	GGAGLGNNQGS(p)	2	1010.45	1010.38
295–308	GGAGLGNNQGS(p)NMG	2	1329.24	1328.48
301–311	NNQGS(p)NMGGGM(ox)	1	1160.60	1160.36
336–345	MMGMLAS(p)QQ	2	1189.72	1189.43
340–347	LASQQNQS(p)	2	952.61	954.38
347–354	SGPS(p)GNN	1	839.62	839.28
364–369	NQAFGS(p)	1	703.56	702.24
369–380	SGNNSYS(p)GSNS	2	1209.19	1209.39
369–380	SGNNSYSGS(p)NS(p)	2	1289.47	1289.36
385–394	WGS(p)AS(p)NAGS(p)	2	1075.07	1075.25
385–396	WGSAS(p)NAGS(p)GSG	2	1196.59	1196.35
387–397	SASNAGS(p)GSGF	2	1020.59	1020.35
391–405	AGS(p)GS(p)GFNGGFGS(p)S(p)M	2	1638.71	1638.39
393–401	SGS(p)GFNGGF	2	906.77	908.31
393–401	S(p)GSGFNGGF	2	907.44	908.31
395–405	SGFNGGFGSS(p)M	2	1126.61	1126.38
397–405	FNGGFGS(p)	2	765.47	765.25
400–410	GFGSS(p)MDSKSS	2	1185.55	1184.41
405–414	MDS(p)KS(p)S(p)GWGM(ox)	2	1340.04	1340.33

p, phosphorylation; ox, oxidation.

washed with 80 mM CaCl$_2$. After centrifugation as described above, the washing solution was removed. The pellet was dissolved in 20 µl of 5% formic acid and applied to the LXQ LC–MS/MS as described above.

Results

Recombinant TDP-43 was phosphorylated with CK1 and the products were purified by means of SDS–PAGE as described [7]. Phosphorylated TDP-43 was digested in the gel with trypsin, chymotrypsin and thermolysin. On LC–MS/MS analysis with LXQ, 18, 6, and 23 phosphorylated peptides were obtained from the trypsin, chymotrypsin, and thermolysin digests, respectively (Table 1). MS/MS analysis data for two representative peptides are shown in Fig. 1. A sequence coverage of 98% was achieved for TDP-43; residues 80–82 and 264–270 were not covered (data not shown).

We identified 29 phosphorylation sites, including the previously reported Ser 91 and Ser 92 [11], as shown in Fig. 2. Interestingly, 18 of these sites were located in the C-terminal glycine-rich region (274–414) of TDP-43 (Fig. 2).

The NetPhosK 1.0 server produces neural network-based predictions of kinase-specific eukaryotic protein phosphorylation sites [12,13]. Prediction scores of CK1 phosphorylation for all serine and threonine residues in TDP-43 were calculated with this server. The scores and the actual phosphorylated sites identified as described above are summarized in Table 2. Although no significant difference of the distribution of the prediction score was seen between the 1–273 region and the 274–414 region (C-terminal Gly-rich region), CK1 clearly phosphorylated more serine/threonine residues in the 274–414 region. In particular, 12 of 14 resides in the low score range (0.36–0.39) were phosphorylated in the 274–414 region, comparing with 6 of 27 residues in the 1–273 region.
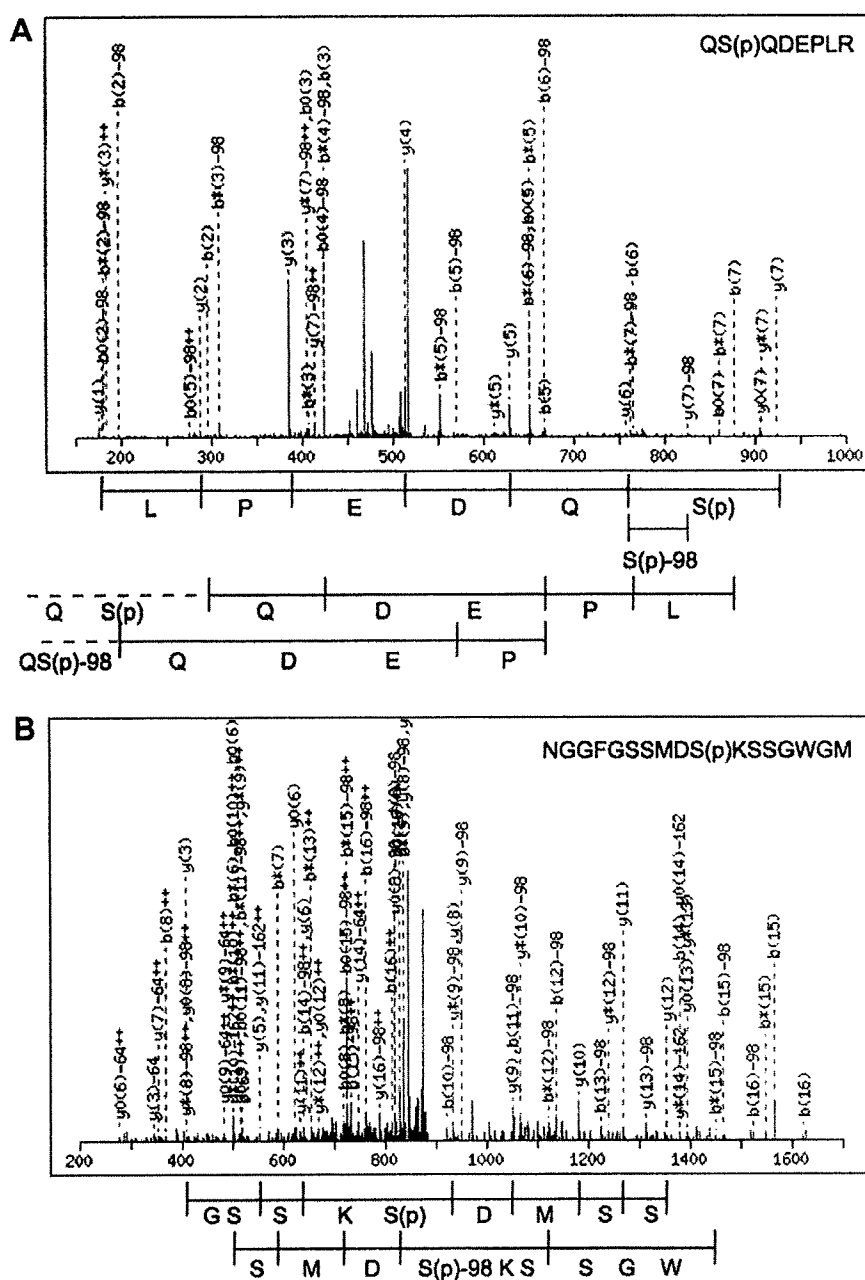

Fig. 1. Identification of phosphorylation sites by LC–MS/MS analysis. (A) Tryptic peptide, QSQDEPLR. The second Ser residue was phosphorylated. (B) Chymotryptic peptide, NGGFGGSSMDSKSSGWGM. The eleventh Ser residue was phosphorylated.
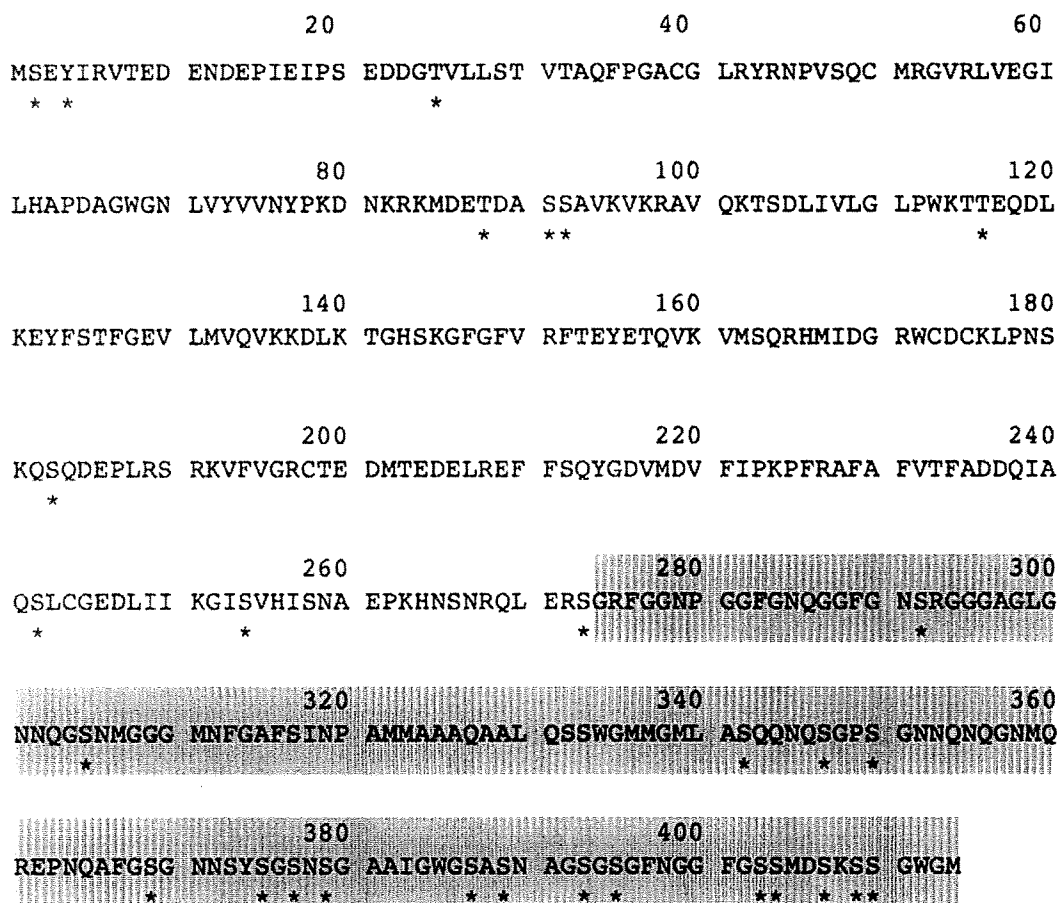
```
                 20                        40                        60

        MSEYIRVTED ENDEPIEIPS EDDGTVLLST VTAQFPGACG LRYRNPVSQC MRGVRLVEGI
        *  *                    *


                 80                       100                       120

        LHAPDAGWGN LVYVVNYPKD NKRKMDETDA SSAVKVKRAV QKTSDLIVLG LPWKTTEQDL
                              *         * *                              *


                140                       160                       180

        KEYFSTFGEV LMVQVKKDLK TGHSKGFGFV RFTEYETQVK VMSQRHMIDG RWCDCKLPNS


                200                       220                       240

        KQSQDEPLRS RKVFVGRCTE DMTEDELREF FSQYGDVMDV FIPKPFRAFA FVTFADDQIA
        *


                260                       280                       300

        QSLCGEDLII KGISVHISNA EPKHNSNRQL ERSGRFGGNP GGFGNQGGFG NSRGGGAGLG
        *          *                    *                               *


                320                       340                       360

        NNQGSNMGGG MNFGAFSINP AMMAAAQAAL QSSWGMMGML ASQQNQSGPS GNNQNQGNMQ
        *                             *         *  *


                380                       400

        REPNQAFGSG NNSYSGSNSG AAIGWGSASN AGSGSGFNGG FGSSMDSKSS GWGM
                *             *  *  *        *  *      *  *       **  *  **
```

Fig. 2. CK1 phosphorylation sites on recombinant TDP-43. Asterisks show phosphorylation sites. The boxed region is the C-terminal Gly-rich region (273–414).

Table 2
The summarized table of prediction scores of CK1 phosphorylation and actual phosphorylated residues (number of phosphorylated residues/number of Ser/Thr residues).

Prediction score range	1–273	274–414 (Gly-rich region)
0.50–0.51	0	1/1
0.40–0.49	4/7	5/7
0.36–0.39	6/27	12/14

Discussion

In this experiment, we identified 29 phosphorylation sites in recombinant TDP-43, including the previously reported Ser 91 and Ser 92 [11]. In particular, 18 of them were located in the C-terminal Gly-rich region. This suggests that the C-terminal Gly-rich region has a conformation that is favorable for CK1 phosphorylation. Interestingly, among 13 pathogenic mutations (G290A, G294V, G298S, A315T, S332N, M337V, Q343R, N345K, G348C, N352S, S379P, A382T, and I383V) found in familial ALS cases and 15 variants (D169G, N267S, G287S, G294A, G295S, G295R, Q331K, G335D, G348C, R361S, S379C, A382T, N390D, N390S, and S393L) found in single sporadic ALS cases [14–21], most are located in the C-terminal Gly-rich region.

The C-terminal Gly-rich region of TDP-43 regulates the alternative splicing of several genes [22,23] and functions as a transcriptional repressor [24]. This domain also binds several heterogeneous nuclear ribonucleoproteins [2,25]. Furthermore, using a yeast TDP-43 proteinopathy model, it was shown that the C-terminal Gly-rich region is required for TDP-43 aggregation and cellular toxicity in vivo [26].

Therefore, phosphorylation and/or mutation of amino acid residue(s) in the C-terminal Gly-rich region of TDP-43 may significantly affect cellular function.

Previously, we reported that recombinant TDP-43 hyperphosphorylated with CK1 showed similar electrophoretic mobility to abnormally phosphorylated TDP-43 observed in the brains of patients with FTLD-U and ALS, and we suggested that CK1 was involved in the abnormal phosphorylation of TDP-43 [7,8]. We prepared 39 antibodies to predicted phosphorylation sites in TDP-43 [7]. Twenty-three of these predicted sites were found to be actually phosphorylated in vitro by CK1. Furthermore, 10 antibodies against actual phosphorylated sites, pS91, pS379, pS389, pS395, pS403, pS404, p403/404, pS409, p410 and pS409/410, were found to label hyperphosphorylated recombinant TDP-43, not non-phosphorylated recombinant TDP-43 [7,8,unpublished data]. Therefore, the specificity of these antibodies was confirmed.

Antibodies raised against Ser 379, Ser 403/404 and Ser 409/410 sites in the C-terminal Gly-rich region labeled TDP-43 accumulations and/or inclusion bodies in brains of patients with FTLD-U and ALS; they also recognized abnormally phosphorylated TDP-43 in the Sarkosyl-insoluble fractions from FTLD-U and ALS brains, and labeled abnormal fibers of 15 nm diameter in inclusion bodies in the spinal cord of ALS patients [7,8]. Furthermore, these antibodies recognized high-molecular-weight smearing, abnormally phosphorylated TDP-43 with a molecular weight of 45 kDa, and C-terminal fragments with molecular weights of 18–28 kDa in Sarkosyl-insoluble fractions from FTLD-U and ALS brain [7,8]. Therefore, at least the Ser 379, Ser 403/404 and Ser 409/410 sites in the C-terminal Gly-rich region, which were identified as in vivo targets of CK1 phosphorylation, may be abnormally phosphorylated in

FTLD-U and ALS brains. Recently, rat monoclonal antibodies raised against phosphorylated Ser 409/410 gave similar results [27], supporting our previous findings. Thus, abnormal phosphorylation of the C-terminal Gly-rich region of TDP-43 is a consistent feature of pathologic inclusions in FTLD-U and ALS brains [7,8,27], and may play a significant role in the cytoplasmic accumulation and the formation of inclusion bodies, as in the cases of tauopathy and alpha-synucleinopathy [28,29].

In summary, our results suggest that multiple Ser residues in the C-terminal Gly-rich region of TDP-43 are major CK1 phosphorylation targets. Furthermore, phosphorylation of Ser 379, Ser 403/404 and Ser 409/410, which we observed previously in TDP-43 accumulated in FTLD-U and ALS brains [7], is also mediated by CK1, indicating that CK1 may be involved in pathological phosphorylation of TDP-43 in vivo. The data on phosphorylation sites of TDP-43 presented here should be useful for further studies on the mechanism of TDP-43 proteinopathy.

Acknowledgments

References

[1] S.H. Ou, F. Wu, D. Harrich, L.F. Garcia-Martinez, R.B. Gaynor, Cloning and characterization of a novel cellular protein, TDP-43, that binds to human immunodeficiency virus type 1 TAR DNA sequence motifs, J. Virol. 69 (1995) 3584–3596.

[2] H.-Y. Wang, I.F. Wang, J. Bose, C.K.J. Shen, Structural diversity and functional implications of the eukaryotic TDP gene family, Genomics 83 (2004) 130–139.

[3] E. Buratti, T. Dork, E. Zuccato, F. Pagani, M. Romano, F.E. Baralle, Nuclear factor TDP-43 and SR proteins promote in vitro and in vivo CFTR exon 9 skipping, EMBO J. 20 (2001) 1774–1784.

[4] J.K. Bose, I.F. Wang, L. Hung, W.-Y. Tarn, C.K.J. Shen, TDP-43 overexpression enhances exon-7 inclusion during SMN Pre-mRNA splicing, J. Biol. Chem. 283 (2008) 28852–28859.

[5] M. Neumann, D.M. Sampathu, L.K. Kwong, A.C. Truax, M.C. Micsenyi, T.T. Chou, J. Bruce, T. Schuck, M. Grossman, C.M. Clark, L.F. McCluskey, B.L. Miller, E. Masliah, I.R. Mackenzie, H. Feldman, W. Feiden, H.A. Kretzschmar, J.Q. Trojanowski, V.M.Y. Lee, Ubiquitinated TDP-43 in frontotemporal lobar degeneration and amyotrophic lateral sclerosis, Science 314 (2006) 130–133.

[6] T. Arai, M. Hasegawa, H. Akiyama, K. Ikeda, T. Nonaka, H. Mori, D. Mann, K. Tsuchiya, M. Yoshida, Y. Hashizume, T. Oda, TDP-43 is a component of ubiquitin-positive tau-negative inclusions in frontotemporal lobar degeneration and amyotrophic lateral sclerosis, Biochem. Biophys. Res. Commun. 351 (2006) 602–611.

[7] M. Hasegawa, T. Arai, T. Nonaka, F. Kametani, M. Yoshida, Y. Hashizume, H.G. Beach, E. Buratti, F.E. Baralle, M. Morita, I. Nakano, A. Oda, K. Tsuchiya, H. Akiyama, Phosphorylated TDP-43 in frontotemporal lobar degeneration and amyotrophic lateral sclerosis, Ann. Neurol. 64 (2008) 60–70.

[8] Y. Inukai, T. Nonaka, T. Arai, M. Yoshida, Y. Hashizume, T.G. Beach, E. Buratti, F.E. Baralle, H. Akiyama, S. Hisanaga, M. Hasegawa, Abnormal phosphorylation of Ser409/410 of TDP-43 in FTLD-U and ALS, FEBS Lett. 582 (2008) 2899–2904.

[9] T. Nonaka, T. Arai, E. Buratti, F.E. Baralle, H. Akiyama, M. Hasegawa, Phosphorylated and ubiquitinated TDP-43 pathological inclusions in ALS and FTLD-U are recapitulated in SH-SY5Y cells, FEBS Lett. 583 (2009) 394–400.

[10] X. Zhang, J. Ye, O.N. Jensen, P. Roepstorff, Highly efficient phosphopeptide enrichment by calcium phosphate precipitation combined with subsequent IMAC enrichment, Mol. Cell. Proteomics 6 (2007) 2032–2042.

[11] J.V. Olsen, B. Blagoev, F. Gnad, B. Macek, C. Kumar, P. Mortensen, M. Mann, Global, in vivo and site-specific phosphorylation dynamics in signaling networks, Cell 127 (2006) 635–648.

[12] N. Blom, T. Sicheritz-Ponten, R. Gupta, S. Gammeltoft, S. Brunak, Prediction of post-translational glycosylation and phosphorylation of proteins from the amino acid sequence, Proteomics 4 (2004) 1633–1649.

[13] NetPhosK server. Available from: http://www.cbs.dtu.dk/services/NetPhosK/.

[14] M.A. Gitcho, R.H. Baloh, S. Chakraverty, K. Mayo, J.B. Norton, D. Levitch, K.J. Hatanpaa, C.L. White 3rd, E.H. Bigio, R. Caselli, M. Baker, M.T. Al-Lozi, J.C. Morris, A. Pestronk, R. Rademakers, A.M. Goate, N.J. Cairns, TDP-43 A315T mutation in familial motor neuron disease, Ann. Neurol. 63 (2008) 535–538.

[15] J. Sreedharan, I.P. Blair, V.B. Tripathi, X. Hu, C. Vance, B. Rogelj, S. Ackerley, J.C. Durnall, K.L. Williams, E. Buratti, F. Baralle, J. de Belleroche, J.D. Mitchell, P.N. Leigh, A. Al-Chalabi, C.C. Miller, G. Nicholson, C.E. Shaw, TDP-43 mutations in familial and sporadic amyotrophic lateral sclerosis, Science 319 (2008) 1668–1672.

[16] E. Kabashi, P.N. Valdmanis, P. Dion, D. Spiegelman, B.J. McConkey, C.V. Velde, J.-P. Bouchard, L. Lacomblez, K. Pochigaeva, F. Salachas, P.-F. Pradat, W. Camu, V. Meininger, N. Dupre, G.A. Rouleau, TARDBP mutations in individuals with sporadic and familial amyotrophic lateral sclerosis, Nat. Genet. 40 (2008) 572–574.

[17] V.M. Van Deerlin, J.B. Leverenz, L.M. Bekris, T.D. Bird, W. Yuan, L.B. Elman, D. Clay, E.M. Wood, A.S. Chen-Plotkin, M. Martinez-Lage, E. Steinbart, L. McCluskey, M. Grossman, M. Neumann, I.L. Wu, W.-S. Yang, R. Kalb, D.R. Galasko, T.J. Montine, J.Q. Trojanowski, V.M.Y. Lee, G.D. Schellenberg, C.-E. Yu, TARDBP mutations in amyotrophic lateral sclerosis with TDP-43 neuropathology: a genetic and histopathological analysis, Lancet Neurol. 7 (2008) 409–416.

[18] A. Yokoseki, A. Shiga, C.-F. Tan, A. Tagawa, H. Kaneko, A. Koyama, H. Eguchi, A. Tsujino, T. Ikeuchi, A. Kakita, K. Okamoto, M. Nishizawa, H. Takahashi, O. Onodera, TDP-43 mutation in familial amyotrophic lateral sclerosis, Ann. Neurol. 63 (2008) 538–542.

[19] N.J. Rutherford, Y.-J. Zhang, M. Baker, J.M. Gass, N.A. Finch, Y.-F. Xu, H. Stewart, B.J. Kelley, K. Kuntz, R.J.P. Crook, J. Sreedharan, C. Vance, E. Sorenson, C. Lippa, E.H. Bigio, D.H. Geschwind, D.S. Knopman, H. Mitsumoto, R.C. Petersen, N.R. Cashman, M. Hutton, C.E. Shaw, K.B. Boylan, B. Boeve, N.R. Graff-Radford, Z.K. Wszolek, R.J. Caselli, D.W. Dickson, I.R. Mackenzie, L. Petrucelli, R. Rademakers, Novel mutations in TARDBP (TDP-43) in patients with familial amyotrophic lateral sclerosis, PLoS Genet. 4 (2008) e1000193.

[20] P. Kuhnlein, A.D. Sperfeld, B. Vanmassenhove, V. Van Deerlin, V.M. Lee, J.Q. Trojanowski, H.A. Kretzschmar, A.C. Ludolph, M. Neumann, Two German kindreds with familial amyotrophic lateral sclerosis due to TARDBP mutations, Arch. Neurol. 65 (2008) 1185–1189.

[21] L. Corrado, A. Ratti, C. Gellera, E. Buratti, B. Castellotti, Y. Carlomagno, N. Ticozzi, L. Mazzini, L. Testa, F. Taroni, F.E. Baralle, V. Silani, S.D. Alfonso, High frequency of TARDBP gene mutations in Italian patients with amyotrophic lateral sclerosis, Hum. Mutat., 2009, doi:10.1002/humu.20950.

[22] Y.M. Ayala, S. Pantano, A. D'Ambrogio, E. Buratti, A. Brindisi, C. Marchetti, M. Romano, F.E. Baralle, Human, Drosophila, and C. elegans TDP43: nucleic acid binding properties and splicing regulatory function, J. Mol. Biol. 348 (2005) 575–588.

[23] P.A. Mercado, Y.M. Ayala, M. Romano, E. Buratti, F.E. Baralle, Depletion of TDP 43 overrides the need for exonic and intronic splicing enhancers in the human apoA-II gene, Nucl. Acids Res. 33 (2005) 6000–6010.

[24] M.M. Abhyankar, C. Urekar, P.P. Reddi, A novel CpG-free vertebrate insulator silences the testis-specific SP-10 gene in somatic tissues: role for TDP-43 in insulator function, J. Biol. Chem. 282 (2007) 36143–36154.

[25] E. Buratti, A. Brindisi, M. Giombi, S. Tisminetzky, Y.M. Ayala, F.E. Baralle, TDP-43 binds heterogeneous nuclear ribonucleoprotein A/B through its C-terminal tail: an important region for the inhibition of cystic fibrosis transmembrane conductance regulator exon 9 splicing, J. Biol. Chem. 280 (2005) 37572–37584.

[26] B.S. Johnson, J.M. McCaffery, S. Lindquist, A.D. Gitler, A yeast TDP-43 proteinopathy model: exploring the molecular determinants of TDP-43 aggregation and cellular toxicity, Proc. Natl. Acad. Sci. USA 105 (2008) 6439–6444.

[27] M. Neumann, L.K. Kwong, E.B. Lee, E. Kremmer, A. Flatley, Y. Xu, M.S. Forman, D. Troost, H.A. Kretzschmar, J.Q. Trojanowski, V.M. Lee, Phosphorylation of S409/410 of TDP-43 is a consistent feature in all sporadic and familial forms of TDP-43 proteinopathies, Acta Neuropathol. 117 (2009) 137–149.

[28] M. Hasegawa, R. Jakes, R.A. Crowther, V.M.Y. Lee, Y. Ihara, M. Goedert, Characterization of mAb AP422, a novel phosphorylation-dependent monoclonal antibody against tau protein, FEBS Lett. 384 (1996) 25–30.

[29] H. Fujiwara, M. Hasegawa, N. Dohmae, A. Kawashima, E. Masliah, M.S. Goldberg, J. Shen, K. Takio, T. Iwatsubo, alpha-Synuclein is phosphorylated in synucleinopathy lesions, Nat. Cell Biol. 4 (2002) 160–164.

Japanese encephalitis – serial CT findings and neuropathology in an autopsy case

Z. Kobayashi[1,2], K. Tsuchiya[2,3] O. Yokota[2,4], C. Haga[2], T. Arai[2], H. Akiyama[2], M. Kotera[5] and H. Mizusawa[1]

[1]Department of Neurology and Neurological Science, Graduate School, Tokyo Medical and Dental University, Tokyo, [2]Tokyo Institute of Psychiatry, [3]Department of Laboratory Medicine and Pathology, Tokyo Metropolitan Matsuzawa Hospital, Tokyo, [4]Department of Neuropsychiatry, Okayama University Graduate School of Medicine, Dentistry and Pharmaceutical Sciences, Okayama, and [5]Department of Neurology, Tsuchiura Kyodo Hospital, Tsuchiura Ibaraki, Japan

Abstract. The patient was a 17-year-old man, who developed Japanese encephalitis in the autumn of 1990 in Japan. He was admitted to our hospital 4 days after onset because of consciousness disturbance. On admission, neurological examination demonstrated left hemiparesis, neck stiffness, and Kernig's sign. He developed generalized tonico-clonic seizure, and required a respirator on the next day of admission. Brain CT 10 days after onset demonstrated hypodensities in the right hippocampus, and the CT obtained 39 days after onset showed whole brain atrophy and hypodensities in the anterior portion of the bilateral thalamus. He died 40 days after onset. Postmortem examination demonstrated perivascular and parenchymal infiltration of lymphocytes and macrophages, proliferation of microglia and astrocytes, and necrosis in the gray matter of the brain. Involvement of the hippocampus and thalamus on CT seemed to reflect the severe lesions characterized by cellular infiltration and necrosis. We discussed for the first time the correlation of CT and neuropathological findings in a patient with Japanese encephalitis.

Introduction

Japanese encephalitis (JE) is a mosquito-borne viral infection caused by neurotropic virus. Pigs are known to be amplifying hosts and transmit the virus. JE is now a major public problem in Southeast Asia with around 50,000 cases and 10,000 deaths per year [Diagana et al. 2007]. In contrast, the incidence of JE in Japan has been less than 10 patients per year [Arai et al. 2008], and one of the reasons for this is thought to be the wide-spread JE virus vaccination of children. Brain images demonstrate abnormalities in the thalamus, hippocampus, substantia nigra and neocortex [Diagana et al. 2007, Handique et al. 2006, Kalita et al. 2000, Misra et al. 1994, Prakash et al. 2004, Shoji et al. 1990]. Here, we report serial CT findings and neuropathology in a patient with JE.

Case report

The patient was a 17-year-old Brazilian, who had come to Japan from Brazil in June 1990. There was no past medical history. In September 1990, he developed fever, headache, and repeated vomiting, and consulted a nearby clinic next day. Domperidone was given by intravenous injection; however, the symptoms were not resolved. On Day 4, he demonstrated consciousness disturbance and was admitted to our hospital. On admission, body temperature was 38.4 °C, blood pressure 124/60 mmHg and pulse rate 100. Neurological examination demonstrated disorientation to time, left hemiparesis, neck stiffness and Kernig's sign. On the same day, generalized tonic-clonic seizure occurred, and electroencephalogram showed diffuse δ waves. Blood tests demonstrated white blood count (WBC) of 10,200/mm^3, but others including blood chemistry were within normal limits. Brain CT was within normal limits (Figure 1a,b,c,d). Cerebrospinal fluid (CSF) examination demonstrated cell count of 648/mm^3 (mononuclear cells 431, polymorphonuclear cells 217), total protein 139
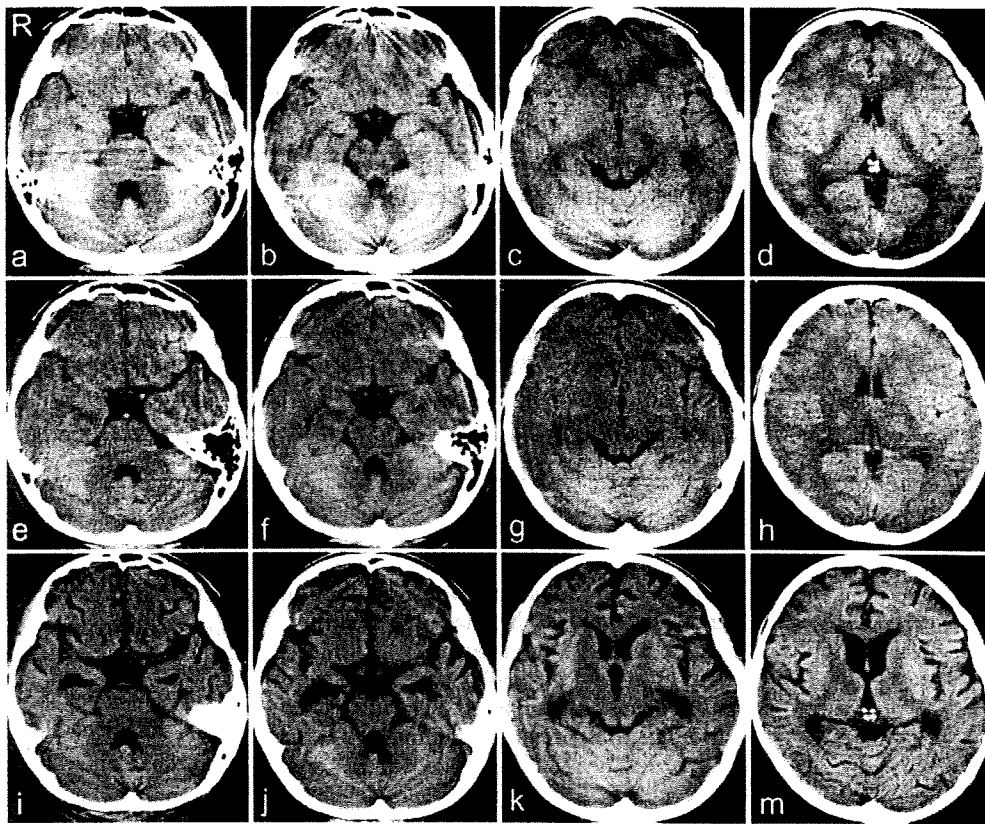
Figure 1. a,b,c,d: Brain CT on admission was within normal limits. e,f,g,h: Brain CT 10 days after onset demonstrated hypodensities in the right hippocampus (e, f), and outlines of the basal ganglia and thalamus were unclear, suggesting edematous changes (g,h) Brain CT obtained 1 day before death disclosed whole brain atrophy and enlargement of the inferior horn of the lateral ventricle with right predominance (i, j). Hypodensities were seen in the anterior portion of the bilateral thalamus (m).

mg/dl and glucose 50 mg/dl (blood sugar 113 mg/dl). He was treated with methylprednisolone pulse therapy with acyclovir and cefuzonam sodium. Bacterial culture of the CSF was negative. The antibody titers of herpes simplex virus (HSV) IgM, varicella zoster virus (VZV) IgM were not detected in the CSF. On the next day of admission, seizures progressed to status epilepticus, and he needed tracheal intubation and a respirator. He gradually presented with decerebrate rigidity after the status epilepticus. On Day 7, hemagglutination inhibition (HI) titer for JE was elevated 1 : 20 (normal range < 1 : 10). Brain CT on Day 10 demonstrated hypodensities in the right hippocampus (Figure 1e,f). Outlines of the basal ganglia and thalamus were unclear (Figure 1g,h), suggesting edematous changes. On Day 21, tracheotomy was performed. On Day 23, HI titer for JE was raised to 1 : 80, and he was given a diagnosis of JE. Thereafter, he developed liver dysfunction. On Day 39, brain CT showed whole brain atrophy and enlargement

of the inferior horn of the lateral ventricle with right predominance (Figure 1i,j). Hypodensities were seen in the anterior portion of the bilateral thalamus (Figure 1m). He died on Day 40 due to exacerbation of liver dysfunction.

Postmortem examination demonstrated bronchopneumonitis and hepatomegaly with dilatation of hepatic veins. The liver weight was 2,270 g. The lungs, duodenum, adrenal glands and kidneys were congestive. Hemorrhage was seen in the duodenum. Atelectasis was seen in the left lung. The left pleural effusion was seen, and the amount was 1,200 ml.

Brain weight was 1,410 g. Mild subarachnoid hemorrhage was seen in the bilateral sylvian fissure. Leptomeninges were unremarkable. Uncal or cerebellar herniation was not seen. Macroscopically, tissue softening was seen in the bilateral thalamus. The subiculum and CA1 of the right hippocampus appeared gray. Pallor of the substantia nigra was evident (Figure 2a).

Brain tissue samples were fixed postmortem with 10% formalin and embedded in par-
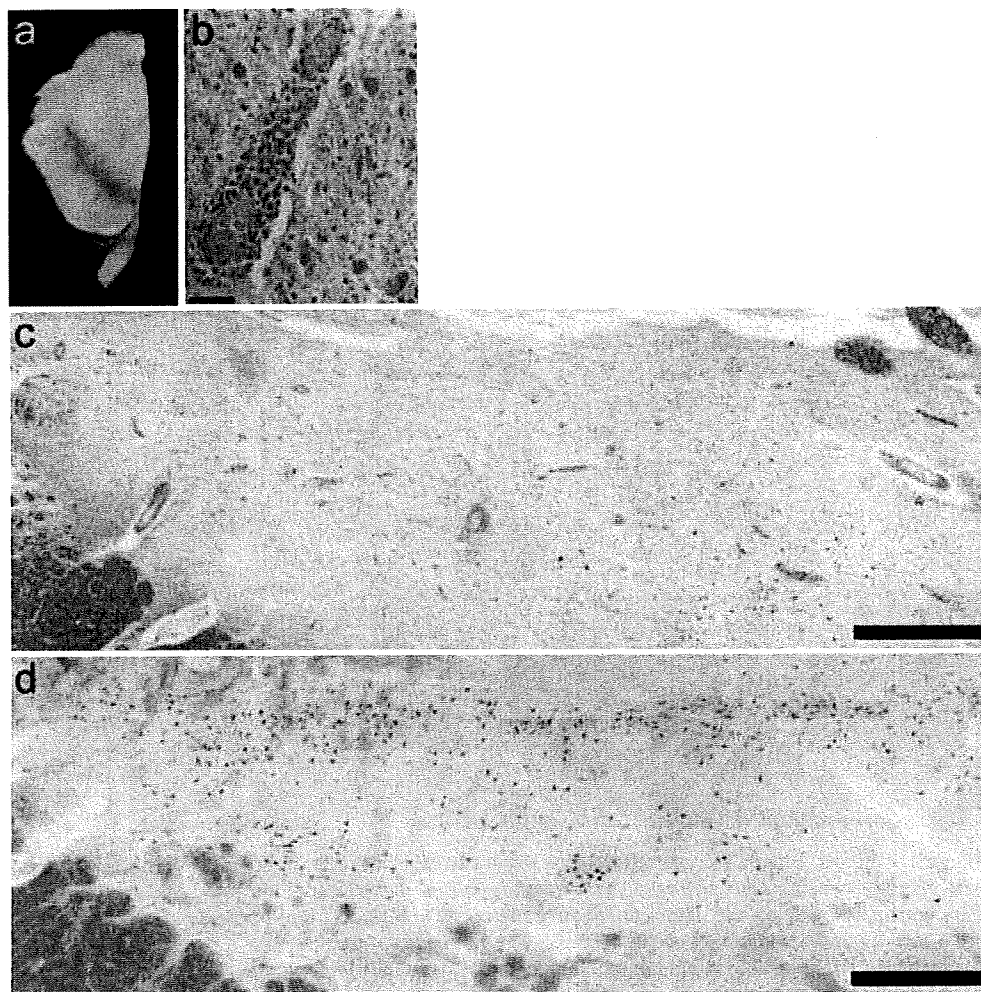
Figure 2. a: Pallor of the right substantia nigra was evident. b: Perivascular cellular infiltration was seen in the substantia nigra. Infiltrating cells consisted of lymphocytes, and macrophages containing melanine. c: Pigmented neurons were lost. d: Substantia nigra of the normal control (46-year-old man) is shown for comparison. Scale bar b: 50 μm; c,d: 1 mm; b: HE stain; c,d: KB stain.

affin. 10 μm thick hemispheric sections were prepared at the plane of the right frontal cortex rostral to the corpus callosum, right caudate head, left mamillary body, right subthalamic nucleus, left lateral geniculate body, right pulvinar nucleus, right parietal cortex and left occipital cortex. The sections of middle portion of the right midbrain, lower portion of the left midbrain, upper and middle portions of the left pons, bilateral cerebellum, upper and middle portions of the medulla oblongata were also prepared. These sections were stained with hematoxyline-eosin (HE) and Klüver-Barrera (KB). Immunohistochemistry using anti-CD3 (T cell marker, SP3, rabbit, monoclonal, 1 : 500, Nichirei), anti-CD20 (B cell marker, L26, mouse, monoclonal, 1 : 100, Dako), anti-CD68 (macrohage/microglia marker, KP1, mouse, monoclonal, 1 : 100,

Dako), and anti-glial fibrillary acidic protein (GFAP) (astrocyte marker, rabbit, polyclonal, 1 : 1,000, Dako) antibodies was also performed.

Microscopically, perivascular and parenchymal infiltration of lymphocytes and macrophages, proliferation of microglia and astrocytes, and neuronal loss were seen in the substantia nigra (Figure 2), hippocampus (Figure 3), parahippocampal gyrus, thalamus (Figure 4a), caudate head, striatum and neocortex (Figure 4b,c,d). Necrotic lesions were seen in the hippocampus (Figure 3a), thalamus (Figure 4a) and neocortex. In the hippocampus, pyramidal cells of the subiculum and CA 1-3 were decreased, and microglial nodules were demonstrated (Figure 3c). In the neocortex, territories covering the depth of the sulci showed severe involvement compared to the crest of the gyri. The first, second and third
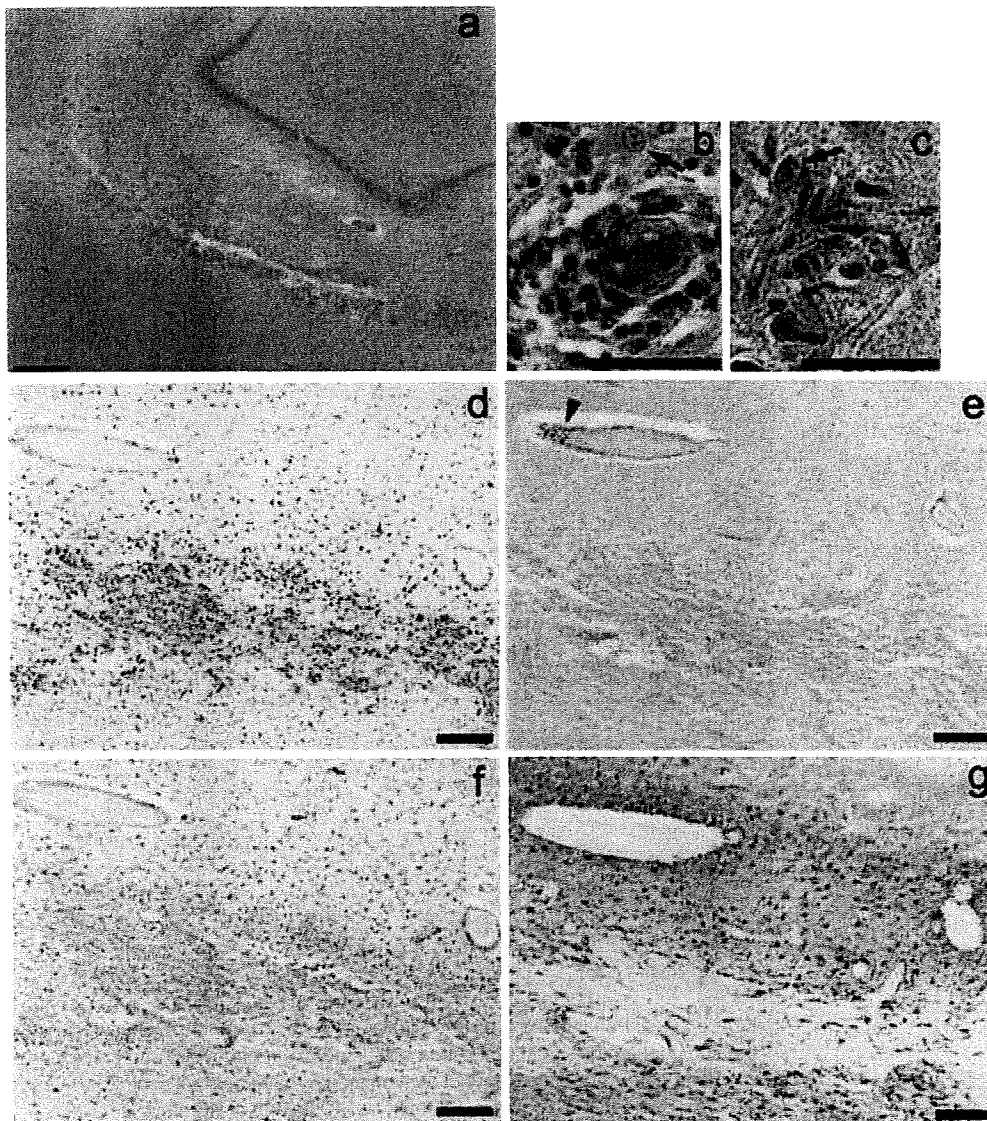
Figure 3. a: Cellular infiltration and necrotic lesions were demonstrated in the subiculum and CA1 of the right hippocampus. b: Perivascular cellular infiltration was seen in the CA1. The arrow indicates a gemistocytic astrocyte. c: Rod-shaped microglia formed a microglial nodule in the CA1. The arrow indicates a neuron. d,e,f,g: are serial sections of the subiculm. d,e,f: Infiltrating cells were CD3-positive cells (d) and CD68-positive cells (f) whereas a few CD20-positive cells were located in the perivascular area (e, arrowhead). g: Astrocytosis was evident around the necrotic lesion. Scale bar a: 500 µm; b,c: 50 µm; d,e,f,g: 200 µm; a,b,c: HE stain; g: GFAP stain.

layer were predominantly involved while all the layers were involved in some parts. The cerebral white matter was spared. Proliferation of microglia and astrocytes without infiltration of lymphocytes or macrophages were seen in the oculomotor nucleus, inferior olivary nucleus, ventral pons, locus ceruleus and dentate nucleus. Purkinje cell loss was evident, but cellular infiltration or glial reaction was not apparent in the cerebellar cortex (Figure 4e). Distribution of brain lesions is shown in Figure 5. In immunohistochemistry, infiltrating cells of the parenchyma were CD3-

positive cells (Figure 3d) and CD68-positive cells (Figure 3f), whereas a few CD20-positive cells were located in the perivascular areas (Figure 3e). Spinal cord was not investigated in this case.

Discussion

In JE, approximately 30% of the patients die, and half of the survivors are left with severe neurological sequelae. Seizures are seen in about 40% of the patient [Solomon et al.
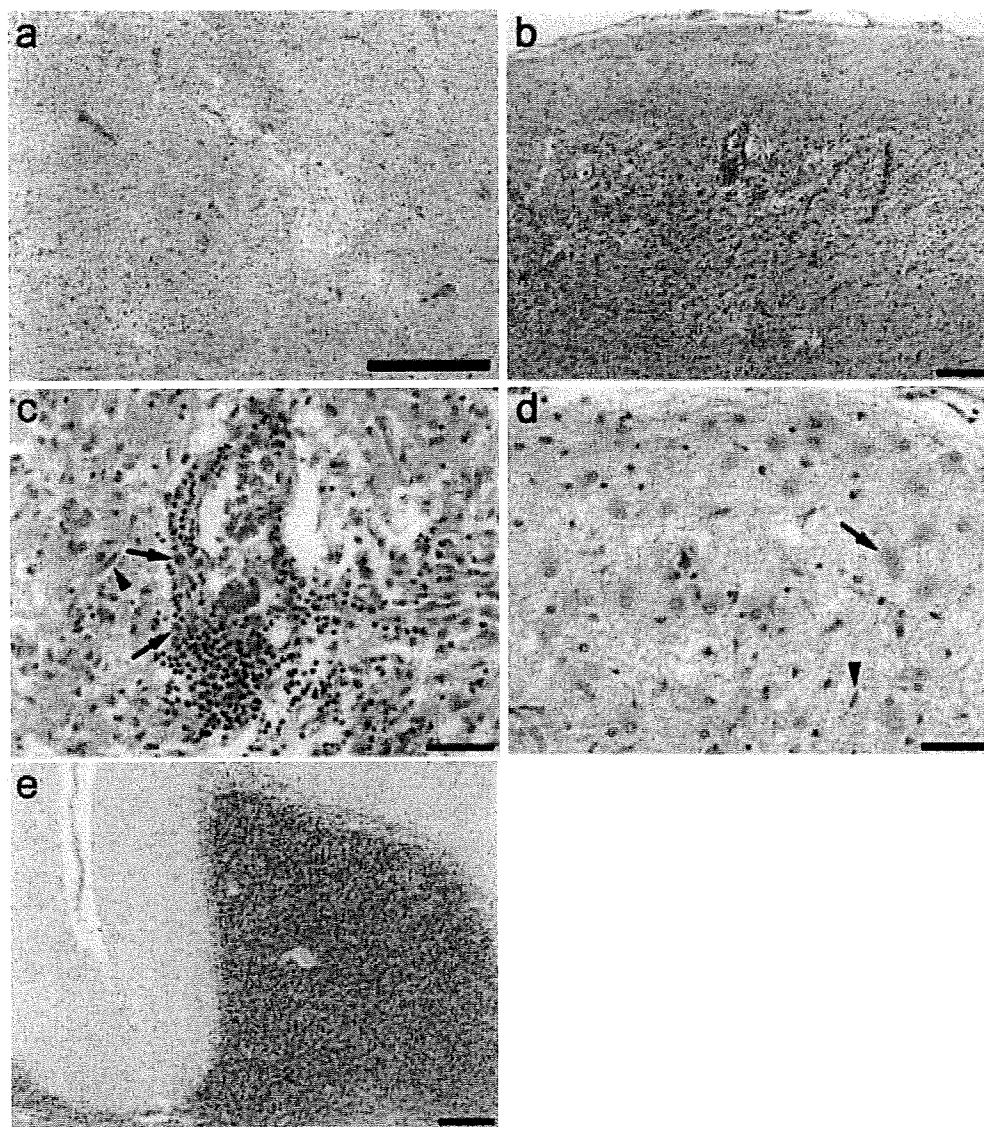
Figure 4.   a: Cellular infiltration and necrotic lesions were seen in the right thalamus. b: Prominent cellular infiltration was demonstrated in the neocortex. c: Perivascular lymphocytic infiltration was seen in the neocortex. The arrows indicate macrophages, and the arrowhead a rod-shaped microglia. d: Gemistocytic astrocytes were seen in the first layer of the neocortex. The arrow indicates a gemistocytic astrocyte, and the arrowhead a rod-shaped microglia. e: Purkinje cells of the cerebellum completely disappeared. Scale bar a: 500 μm; b: 200 μm; c,d: 50 μm; e: 200 μm. a,b,c,d,e: HE stain.

2002]. In the 1950s, approximately 5,000 cases were reported per year in Japan [Matsunaga et al. 2008]. However, the incidence of JE in Japan has decreased, and has been less than 10 patients per year since 1992, in whom the majority of the cases are in the elderly population, probably due to impaired immune responses [Arai et al. 2008]. One of the reasons for this is thought to be due to the widespread JE virus vaccination of children (since 1967). However, routine vaccination has not been recommended by the Japanese government since 2005 because more than 10 cases including some severe cases of acute

disseminated encephalomyelitis (ADEM) after JE vaccination have been reported since 1991 in Japan [Ohya et al. 2007]. This may result in an increased incidence of JE in Japan in the future [Matsunaga et al. 2008].

The presented patient was Brazilian, and had not received a JE virus vaccination. He developed JE about 3 months after he had come to Japan. Usually, patients who die of JE die within 1 week of hospital admission [Hoke et al. 1992, Johnson et al. 1985], so the disease duration of this patient (40 days) was somewhat long. At autopsy, cellular infiltration was demonstrated in the gray matter of
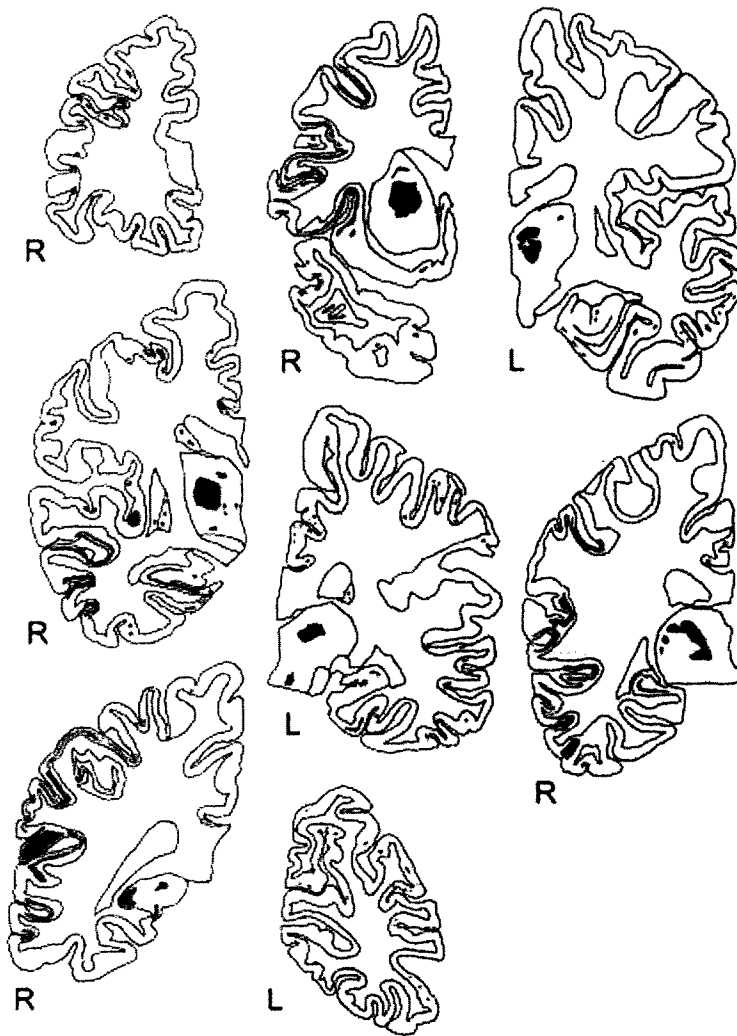
Figure 5a.

Figure 5b.

Figure 5. Distribution of brain lesions disclosed by microscopic examination (cerebrum × 0.8, brainstem and cerebellum × 1.5). We divided the lesions into two groups, consisting of cellular proliferation and necrosis. The proliferating cells were composed of lymphocytes, macrophages, microglia and astrocytes. Cellular proliferations alone were shown in red, and necrotic lesions were shown in dark gray.

the brain. Necrotic lesions were seen in the thalamus, hippocampus and neocortex, indicating severe involvement of these regions.

Radiologically, hypodensities of CT in the thalamus [Diagana et al. 2007, Kalita et al. 2000, Shoji et al. 1990] and hippocampus [Handique et al. 2006] in JE were previously reported, although CT hardly demonstrated abnormalities of the substantia nigra or neocortex. On the other hand, abnormalities of the substantia nigra are frequently detected on MRI [Kalita et al. 2000, Handique et al. 2006], and those in the neocortex are sometimes demonstrated [Kalita et al. 2000, Prakash et al. 2004]. Furthermore, involvement of amygdala, uncus, basal ganglia, pons, or cerebellum is also demonstrated in some cases [Handique et al. 2006, Kalita et al. 2000]. Thalamic lesions are sometimes hemorrhagic [Diagana et al. 2007, Misra et al. 1994].

Recently, MRI abnormalities have been increasingly reported in postictal patients with generalized seizures or status epilepticus [Parmar et al. 2006]. Abnormalities are frequently seen in the hippocampus and include changes of signal intensities and subsequent atrophy. Seizure activity leads to a 2- to 3-fold increase in cerebral metabolic rate of oxygen and glucose, and hippocampus is thought to be vulnerable to the relative hypoxia related to seizure. Histopathologically, neuronal loss and reactive gliosis are seen not only in the hippocampus, but also in the amygdala, dorsomedial thalamic nucleus and Purkinje cell layer of the cerebellum [Fujikawa et al. 2000]. Abnormalities in the hippocampus on CT or MRI seen in JE patients with seizures may be partly due to, in fact, secondly changes following seizures.

In JE, neuropathologically, clusters of petechiae are found in the brain [Zimmerman 1946]. Focal infiltrations of mononuclear cells are demonstrated in the meninges [Lewis et al. 1947, Zimmerman 1946]. Parenchymal lesions are predominantly seen in the thalamus, substantia nigra, and hippocampus; however, lesions are also seen in the cerebral cortex, basal ganglia, cerebellum, and anterior horn of the spinal cord [Diagana et al. 2007, Shiraki 1966, Zimmerman 1946]. Observed lesions include cellular infiltration in the perivascular area and parenchyma. Phagocytic microglia remove degenerated neurons and form microglial nodules. Purkinje cell

loss had been emphasized as a characteristic feature of JE, but Johnson et al. [1985] described that it was presumably associated with hyperthermia or anoxia because viral antigen was not demonstrated in the Purkinje cells. In our case, Purkinje cell loss may be due to the status epilepticus [Fujikawa et al. 2000], because cellular infiltration was not demonstrated in the cerebellar cortex.

To date, phenotypes of the infiltrating cells have been described in two reports [Iwasaki et al. 1993, Johnson et al. 1985]. Johnson et al. [1985] reported cases in the acute stage (disease duration of 3 – 9 days) and showed perivascular inflammatory responses with a predominance of T cells and small numbers of macrophages. In contrast, inflammatory cells invading the parenchyma were predominantly macrophages with small numbers of T cells. B cells remained localized to perivascular areas. Meanwhile, Iwasaki et al. [1993] reported two cases in the subacute and chronic stage (disease duration of 14 and 76 days, respectively), and showed that more than half of the T cells widely dispersed in the parenchymal tissue distant from perivascular areas. Distribution of the T cells seen in our case resembled to those reported by Iwasaki et al. [1993], probably reflecting the disease duration.

JE virus-specific antigen was reported to be localized in neurons of the affected areas [Desai et al. 1995]. Hippocampus, adjoining temporal cortex, and thalamus often showed a high density of antigen-bearing neurons, followed by midbrain, medulla oblongata and cerebellum. In some cases, the Purkinje cells and granule cells of the cerebellum were immunolabeled for the viral antigen despite the absence of microglial reaction or neuronophagia. In contrast, microglial reaction and neuronophagia were prominent in the cerebellar nuclei, followed by inferior olivary nucleus; many of the microglia being positive for the phagocytosed viral antigen.

To date, both radiological and neuropathological findings in a patient with JE have not been reported. Because status epilepticus was seen in the clinical course in our case, neuronal loss of the hippocampus demonstrated by autopsy may be partly due to the status epilepticus [Fujikawa et al. 2000]. Similarly, the possibility that the hypodensities of the hippocampus on CT had been secondary

changes following the status epilepticus could not be completely excluded.

In conclusion, the CT and neuropathological findings of our case were each consistent with those previously reported in JE. Involvement of the hippocampus and thalamus on CT seemed to reflect the severe lesions characterized by cellular infiltration and necrosis.

Acknowledgment

References

Arai S, Matsunaga Y, Takasaki T, Tanaka-Taya K, Taniguchi K, Okabe N, Kurane I. Vaccine Preventable Diseases Surveillance Program of Japan. Japanese encephalitis: surveillance and elimination effort in Japan from 1982 to 2004. Jpn J Infect Dis. 2008; 61: 333-338.

Desai A, Shankar SK, Ravi V, Chandramuki A, Gourie-Devi M. Japanese encephalitis virus antigen in the human brain and its topographic distribution. Acta Neuropathol. 1995; 89: 368-373.

Diagana M, Preux PM, Dumas M. Japanese encephalitis revisited. J Neurol Sci. 2007; 262: 165-170.

Fujikawa DG, Itabashi HH, Wu A, Shinmei SS. Status epilepticus-induced neuronal loss in humans without systemic complications or epilepsy. Epilepsia. 2000; 41: 981-991.

Handique SK, Das RR, Barman K, Medhi N, Saharia B, Saikia P, Ahmed SA. Temporal lobe involvement in Japanese encephalitis: problems in differential diagnosis. AJNR Am J Neuroradiol. 2006; 27: 1027-1031.

Hoke CH, Vaughn DW, Nisalak A, Intralawan P, Poolsuppasit S, Jongsawas V, Titsyakorn U, Johnson RT. Effect of high-dose dexamethasone on the outcome of acute encephalitis due to Japanese encephalitis virus. J Infect Dis. 1992; 165: 631-637.

Iwasaki Y, Sako K, Tsunoda I, Ohara Y. Phenotypes of mononuclear cell infiltrates in human central nervous system. Acta Neuropathol. 1993; 85: 653-657.

Johnson RT, Burke DS, Elwell M, Leake CJ, Nisalak A, Hoke CH, Lorsomrudee W. Japanese encephalitis: immunocytochemical studies of viral antigen and inflammatory cells in fatal cases. Ann Neurol. 1985; 18: 567-573.

Kalita J, Misra UK. Comparison of CT scan and MRI findings in the diagnosis of Japanese encephalitis. J Neurol Sci. 2000; 174: 3-8.

Lewis L, Taylor HG, Sorem MB, Norcross JW, Kindsvatter VH. Japanese B encephalitis. Clinical observations in an outbreak on Okinawa Shima. Arch Neurol Psychiatry. 1947; 57: 431-463.

Matsunaga T, Shoda M, Konishi E. Japanese encephalitis viral infection remains common in Japan. Pediatr Infect Dis J. 2008; 27: 769-770.

Misra UK, Kalita J, Jain SK, Mathur A. Radiological and neurophysiological changes in Japanese encephalitis. J Neurol Neurosurg Psychiatry. 1994; *57:* 1484-1487.

Ohya T, Nagamitsu S, Yamashita Y, Matsuishi T. Serial magnetic resonance imaging and single photon emission computed tomography study of acute disseminated encephalomyelitis patient after Japanese encephalitis vaccination. Kurume Med J. 2007; *54:* 95-99.

Parmar H, Lim SH, Tan NC, Lim CC. Acute symptomatic seizures and hippocampus damage: DWI and MRS findings. Neurology. 2006; *66:* 1732-1735.

Prakash M, Kumar S, Gupta RK. Diffusion-weighted MR imaging in Japanese encephalitis. J Comput Assist Tomogr. 2004; *28:* 756-761.

Shiraki H. The neuropathology of encephalitis Japonica in humans especially from subchronic to chronic stage. Neuropatol Pol. 1966; *4:* 419-448.

Shoji H, Murakami T, Murai I, Kida H, Sato Y, Kojima K, Abe T, Okudera T. A follow-up study by CT and MRI in 3 cases of Japanese encephalitis. Neuroradiology. 1990; *32:* 215-219.

Solomon T, Dung NM, Kneen R, Thao le TT, Gainsborough M, Nisalak A, Day NP, Kirkham FJ, Vaughn DW, Smith S, White NJ. Seizures and raised intracranial pressure in Vietnamese patients with Japanese encephalitis. Brain. 2002; *125:* 1084-1093.

Zimmerman HM. The pathology of Japanese B encephalitis. Am J Pathol. 1946; *22:* 965-991.

Case Report

Clinicopathological study of early progressive multifocal leukoencephalopathy incidentally found in a schizophrenia patient *

Kenichi Oshima,[1–3] Kuniaki Tsuchiya,[2,4] Kazuhiro Niizato,[1,2] Haruhiko Akiyama,[2] Tetsuaki Arai[2] and Kazuo Nagashima[5]

Department of [1]Psychiatry and [4]Pathology, Tokyo Metropolitan Matsuzawa Hospital, [2]Tokyo Institute of Psychiatry, and [3]Tokyo Metropolitan Center for Mental Health and Welfare, Tokyo, and [5]Department of Pathology, Sapporo Higashi Tokushukai Hospital, Sapporo, Japan

A 58-year-old Japanese man developed psychomotor excitement and hallucinatory paranoia at age 53, which gradually developed to residual schizophrenia. He was administered various common tranquilizers until death. Myelodysplastic syndrome was noted 10 months before death. A routine autopsy was performed. The brain weighed 1365 g, and macroscopic observation revealed no remarkable findings. However, microscopic examination disclosed cells with enlarged and basophilic nuclei, and unusual astrocytes in the demyelinated foci, especially at the corticomedullary junctions in the temporal and occipital lobes. On the other hand, the white matter was relatively intact. Immunohistochemical analysis using anti-JC virus protein, VP-1 antibody, demonstrated JC virus-infected cells in not only abnormal glial cells and neurons but also normal-looking cells, which are suggestive of progressive multifocal leukoencephalopathy (PML). Immunostaining for GFAP revealed severe gliosis and some scattered abnormal enlarged nuclear cells in the lesions. Some clusters of CD8-positive lymphocytes were seen, which kill infected cells. PML could be considered a short-term disease preceding death, as "incidental PML" in this case. This is a rare autopsy case of early PML occurring in a schizophrenia patient with PML.

Key words: clinicopathological study, myelodysplastic syndrome, opportunistic infection, progressive multifocal leukoencephalopathy, schizophrenia.

INTRODUCTION

Progressive multifocal leukoencephalopathy (PML) is a deadly demyelinating disease of the CNS caused by papovavirus and JC virus infection,[1] which occurs almost exclusively in people with severe immune deficiency, that is, it is an opportunistic infection. Progressive dementia, hemiparesis and hemianopsia are the most common clinical manifestations of PML. Rapid deterioration leading to coma and death within a few weeks or months after the onset of symptoms is typical. A change in mentation, which includes personality change, difficulty with memory, emotional lability, and frank dementia, has been the presenting sign in approximately one-third of cases and eventually involves most patients.[2]

This is a rare autopsy report of a schizophrenia patient with early PML. These findings, which were discovered incidentally in a routine autopsy, suggest that the PML pathology manifested in the early phase; therefore, it is essential to report these clinical and immunohistological findings.

CLINICAL COURSE

A 58-year-old Japanese man developed psychomotor excitement and hallucinatory paranoia at age 53. While considering a suicide attempt, he was taken into protective custody by police. He was then admitted to a mental hospital for several months. After discharge, he stopped attending a mental clinic and his mental condition worsened gradually. He was admitted again at age 55 and was hospitalized until death. He was very excited on admission and could not stop speaking. He gradually fell into residual schizophrenia: psychomotor slowing, lack of initiative,

Table 1 Data from inspected blood taken from the case patient in our hospital

					MDS diagnosed by bone marrow aspiration				
Period before death (months)			14	12	10	8	5	3	1
Inspected item	Reference value	Unit	Inspection value						
WBC	45–80	×10²	78	42	77	85	161	278	309
RBC	450–550	×10⁴	317	310	174	189	289	268	267
HGB	13.5–17.5	g/dL	9.8	9.9	5.9	6.3	9.6	8.8	9.1
HCT	40–52	%	31.2	31.3	18.6	19.6	29.2	28.6	30.7
MCV	85–98	Fl	98.4	101	106	103	101	106	115
MCH	29–35	Pg	30.9	31.9	33.9	33.3	33.2	32.8	34.1
MCHC	32–36	g/dL	31.4	31.6	31.7	32.1	32.9	30.8	29.6
PLT	13–30	×10⁴	16.8	25.2	21.4	11.8	22.9	30.6	30.6
NEUT	40–67	%	83.9	65	73	80	81	88	96
LYMPH	25–45	%	8.7	17.9	12	16	15	5	2
MONO	3–6	%	6	8.9	7	2	1	6	2
EOS	2–5	%	1.4	7.7	8	2	3	1	
BASO	0–1	%	0	0.5					
HN					+	+	+		
RBC disparity					++	++	+	+	+
CRP	<0.3	mg/dL	5.9	2.6	0.2	5.4	2	13.5	14.6

BASO, basocyte; EOS, eosinocyte; HCT, hematocrit; HGB, hemoglobin; HN, Hypersegmented neutrophil; LYMPH, lymphocyte; MCH, mean corpuscular hemoglobin; MCHC, mean corpuscular hemoglobin concentration; MCV, mean corpuscular volume; MDS, myelodysplastic syndrome; MONO, monocyte; NEUT, neurtrophil; RBC, red blood cell; WBC, white blood cell.

poverty of speech content, poor nonverbal communication, poor self-care and poor social performance. He was taking tranquilizers during the majority of his admission: risperidone 2 mg/day or haloperidol 5–10 mg/day. He complained of hallucinations continuously; he claimed that his back was being stabbed with needles, and he saw miniature people. Memory disturbance was noted 13 months before death. Cranial CT scan did not demonstrate any remarkable findings. He had weakened physical activity, severe anemia and neutropenia. Myelodysplastic syndrome (MDS) was noted on bone marrow aspiration at 7 months before death (Table 1). Finally, his physical condition declined until he was bedridden at age 57. It was difficult for a clinical physician to assess his psychiatric symptoms, so neurodegenerative diseases were suspected at that time. He died 42 months after admission. The duration of his mental illness was 5 years.

Physical pathological findings

Postmortem examination, performed 2 hours after death, revealed an abscess in the renal pelvis of the right kidney, pneumonia and chronic pancreatitis. Sepsis associated with nephropyelitis was considered the main cause of death.

Neuropathological findings

The fresh brain weighed 1365 g. Serial sections of the formalin-fixed brain revealed slightly bilateral ventricle enlargement. We used paraffin-embedded blocks from the left brain for microscopic examination.

Histopathological findings

HE staining showed many foamy macrophages, hypertrophic astrocytes and abnormal enlarged oligodendrocytes in the corticomedullary junction (Fig. 1A,B). Macrophages and astrocytic gliosis were seen to various degrees. Some isolated lesions, accompanied by severe gliosis in the white matter, contained some vacuolations (Fig. 1G).

KB preparation showed loss of myelin sheaths in the corticomedullary junction of the temporal and occipital lobes (Fig. 2). Affected myelinated fibers of the corticomedullary junction were observed in both white matter and the intracortical region (Fig. 1C,D. The intracortical region was affected more severely than the white matter. The axons were relatively preserved.

Modified Gallyas-Braak staining[3] disclosed a small amount of neurofibrillary tangles in the transentorhinal region (Fig. 1L) (Braak stage I).[4] Silver stain disclosed a small amount of senile plaques in limbic regions (Braak stage B).[4] This case was not compatible with any neurodegenerative diseases.

Immunohistochemical findings

Immunoreactivity for a JC virus protein, VP-1,[5] disclosed infected cells in the corticomedullary junction (Fig. 1E). Oligodendrocytes, neurons and astrocytes were seen to be infected (Fig. 1F). The intracortical region was affected more severely than the white matter. The large confluent
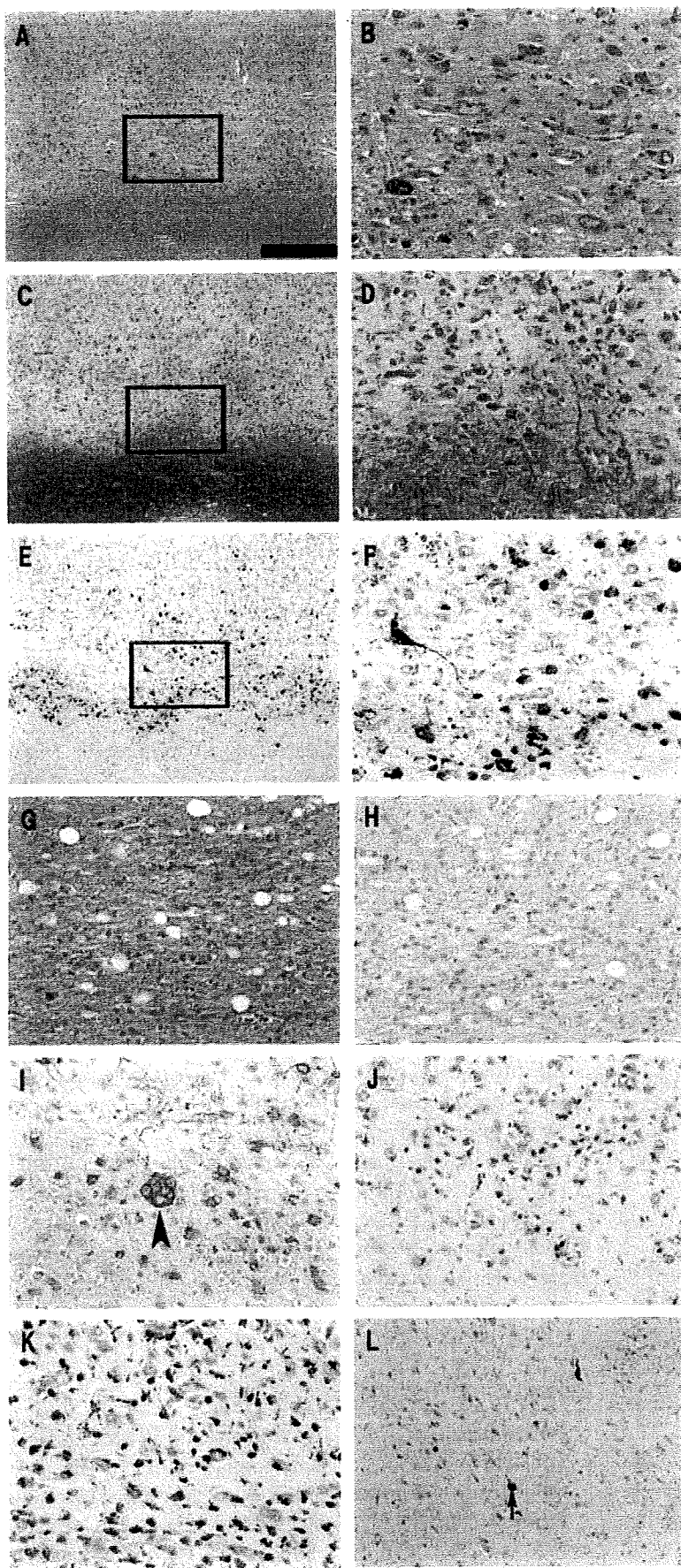
Fig. 1 HE staining showed an eosinophilic area extending in a belt along the corticomedullary junction, which had a different color from the normal surroundings (A). Figures (B), (D) and (F) are respective enlargements of the square in Figures (A), (C) and (E). Abnormal glial cells were seen (B). KB staining showed demyelination in the corticomedullary junctions (C and D). The axons were relatively preserved. Immunohistochemical staining for a JC virus protein, VP-1, showed reactivity along the demyelination region in brown (E). Infected cells throughout the degenerative lesions were seen (F). Not only glial cells but also neurons were positively stained. Isolated demyelinated areas in white matter were seen (G), but immunostaining for VP-1 could not necessarily be revealed in these areas (H). Immunostaining for GFAP revealed gliosis that widely spread to the cortex and white matter in brown. Abnormal nuclei astrocytes (arrow head) were seen (I). CD4-negative and CD8-positive T-cells were seen in some involved areas in brown (J). Numerous CD68-positive macrophages were observed in brown (K). Modified Gallyas-Braak staining showed sparse neurofibrillary tangles in entorhinal and transentorhinal regions in purple (L). Representative bar is in Figure (A): Bar = 400 μm A, C, E. Bar = 200 μm L. Bar = 100 μm B, D, F-K. Staining methods: HE: A, B, G. KB: C, D. Gallyas-Braak: L. Immunostaining (antibodies): VP-1: E, F, H. GFAP: I. CD8: J. CD68: K.
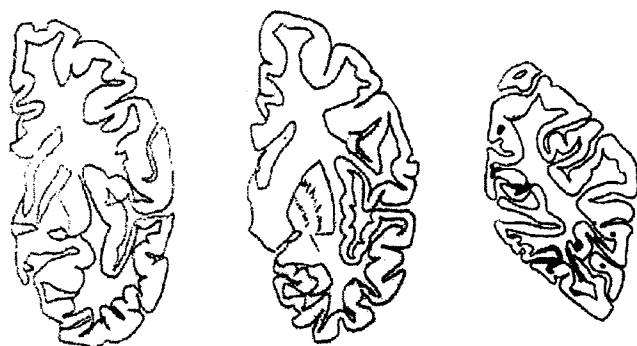
© 2008 Japanese Society of Neuropathology

Fig. 2 This schema shows the distribution of demyelinated areas (red) in KB staining of coronal slice specimens (slice level: left: amygdala, center: pes hippocampi, right: occipital lobe). The involved areas were seen particularly in the corticomedullary junction of the occipital lobe.

lesions contained severely immunopositive abnormal enlarged astrocytes and oligodentroglia (Fig. 1F), which cannot be necessarily detected in isolated small lesions of the white matter (Fig. 1H).

Immunostaining for GFAP (Dako Japan, Kyoto, Japan) revealed gliosis that widely spread to the intracortical region and white matter. Some scattered astrocytes with abnormal enlarged nuclei were seen (Fig. 1I).

Immunostaining disclosed some clusters of lymphocytes that were CD4 negative and CD8 (Nichirei, Tokyo, Japan) positive T-cells (Fig. 1J). Immunostaining for CD20 did not reveal B-cells in the lesions.

Macrophages, which immunostained for CD68 (Dako), were seen in the affected area (Fig. 1K).

Neuropathological diagnosis

Progressive multifocal leukoencephalopathy (PML).

DISCUSSION

Typical symptoms of general PML are diverse and are related to the location and amount of damage in the brain. PML lesions can occur anywhere in the CNS white matter; not only the cerebrum, brainstem, cerebellum, but also the spinal cord can be affected. The progression of deficits leads to life-threatening disability and death within a few weeks or months. The methods to confirm diagnosis are immunohistochemical labeling for JC virus (JCV) protein, revealing the virus by electronic microscopic examination, and revealing mRNA of JCV protein by *in situ* hybridization.[6]

Compared to previous neuropathological reports of PML, the severity of PML in this case was relatively slight. This case can be regarded as an early PML case. The research for early cases may help to define the pathogen-

esis of PML. The involved area of this case was limited to the occipital and temporal lobes. The corticomedullary junction, which can often be infected through blood flow, could be considered one of the frequent onset regions of PML. There are few neuropathological papers about early PML cases. In the early PML case report by Astrom,[7] which was discovered in a routine autopsy, clusters of small, rounded lesions of demyelination with glial changes were located within the restricted areas of white matter. Many lesions were isolated, some were overlapping. The lesions were mostly uniform, that is, small and rounded in the white matter, with positive immunostaining for anti-virus protein. Larger lesions with destruction of myelin along the border between gray and white matter appeared to be the result of confluence of the lesions. They extended along the border over varying distances and involved the adjacent gray and white matter. This could be a typical early PML case. Compared to Astrom's case, in our case the corticomedullary junction was affected, whereas the white matter was relatively preserved. Clusters of CD8-positive lymphocytes were seen in the lesions. CD8-positive lymphocytes are cytotoxic T-cells, which kill cells infected by the virus. In addition, numerous macrophages and glia were seen. The cytokines induced by lymphocytes, macrophages and so on could be related to the progression of PML.

Psychiatric symptoms relating to PML are hard to detect, even retrospectively. The neuropathological involvement in this case, revealed in routine autopsy, could have represented so-called "incidental PML". Orba reported that in 7% of 94 PML cases no immunodeficiency diseases were detected.[8] Previous PML cases, in which immunodeficiency diseases were not detected, have been reported, suggesting "primary PML";[9] however, it is difficult for these cases to be regarded as having a non-opportunistic infection merely because some inspected tests were within normal limits. JCV does not have pathogenicity for general individuals. The mechanism of onset and progression remains unknown. Most PML patients have been reported in an immunosuppressive state accompanied by lymphoma, leukemia, carcinoma, tuberculosis, and especially AIDS. The underlying disease in this case was MDS, which includes a large spectrum of hematological disease with common features characterized by anemia. There have been few case reports of PML associated with MDS.[10,11] PML is still a rare neurological disorder in Japan because AIDS is rare compared to other countries; however, HIV infection appears to be spreading widely in the Japanese population.[12,13] In this case, the patient could not be diagnosed with schizophrenia before the age of 53. Schizophrenia is generally regarded as a disease starting in adolescence and early adulthood; however, the proportion of schizophrenia patients whose illness first emerges after

the age of 40 has been estimated to be 23.5%.[14] In this case, the cognitive decline was considered to have resulted from schizophrenically negative symptoms due to geriatric chronic hospitalization.[15] Clinical physicians could not detect PML in this case and all psychiatric symptoms of this patient may have been considered as relating to schizophrenia. PML may be easily overlooked in severe psychiatric patients. MRI may have revealed the PML in this case. A highly intense area can usually be seen on T2-weighted MRI.[16] There is no known effective cure for PML but, in some cases, the disease slows or stops if the patient's immune system improves; some AIDS patients with PML have been able to survive for several years with the advent of highly active antiretroviral therapy (HAART).[17] Clinical physicians should consider PML in chronic psychiatric patients who are likely to develop opportunistic infection.

In conclusion, a rare autopsy case of early PML occurring in a schizophrenia patient with PML is reported. The corticomedullary junctions of the temporal and occipital lobes were affected, whereas the white matter was relatively preserved. Some clusters of CD8-positive lymphocytes were seen in the lesions.

ACKNOWLEDGMENTS

REFERENCES

1. Padgett BL, Walker DL, ZuRhein GM, Eckroade RJ, Dessel BH. Cultivation of papova-like virus from human brain with progressive multifocal leucoencephalopathy. *Lancet* 1971; **1**: 1257–1260.
2. Major EO, Amemiya K, Tornatore CS, Houff SA, Berger JR. Pathogenesis and molecular biology of progressive multifocal leukoencephalopathy, the JC virus-induced demyelinating disease of the human brain. *Clin Microbiol Rev* 1992; **5**: 49–73.
3. Uchihara T, Kondo H, Ikeda K, Kosaka K. Alzheimer-type pathology in melanin-bleached sections of substantia nigra. *J Neurol* 1995; **242**: 485–489.
4. Braak H, Braak E. Neuropathological stageing of Alzheimer-related changes. *Acta Neuropathol* 1991; **82**: 239–259.
5. Okada Y, Sawa H, Endo S *et al.* Expression of JC virus agnoprotein in progressive multifocal leukoencephalopathy brain. *Acta Neuropathol* 2002; **104**: 130–136.
6. Shintaku M, Matsumoto R, Sawa H, Nagashima K. Infection with JC virus and possible dysplastic ganglion-like transformation of the cerebral cortical neurons in a case of progressive multifocal leukoencephalopathy. *J Neuropathol Exp Neurol* 2000; **59**: 921–929.
7. Astrom KE, Stoner GL. Early pathological changes in progressive multifocal leukoencephalopathy: a report of two asymptomatic cases occurring prior to the AIDS epidemic. *Acta Neuropathol* 1994; **88**: 93–105.
8. Orba Y, Sawa H, Nagashima K. [Molecular neuropathology of JC virus]. *No To Shinkei* 2002; **54**: 101–109.
9. Rockwell D, Ruben FL, Winkelstein A, Mendelow H. Absence of imune deficiencies in a case of progressive multifocal leukoencephalopathy. *Am J Med* 1976; **61**: 433–436.
10. Barber P, Gorst DW, Morris JA, Pearson JD. Progressive multifocal leukoencephalopathy, myelodysplastic syndrome type II and prostatic carcinoma. *Postgrad Med J* 1984; **60**: 157–158.
11. Hequet O, Salles G, Espinousse D *et al.* Multifocal progressive leukoencephalopathy occurring after refractory anemia and multiple infectious disorders consecutive to severe lymphopenia. *Ann Hematol* 2002; **81**: 340–342.
12. Hashimoto S, Kawado M, Murakami Y *et al.* Numbers of people with HIV/AIDS reported and not reported to surveillance in Japan. *J Epidemiol* 2004; **14**: 182–186.
13. Komatsu R, Sawada T. The role of international migration in infectious diseases: the HIV epidemic and its trends in Japan. *Int J Health Serv* 2007; **37**: 745–759.
14. Harris MJ, Jeste DV. Late-onset schizophrenia: an overview. *Schizophr Bull* 1988; **14**: 39–55.
15. Harvey PD, Silverman JM, Mohs RC *et al.* Cognitive decline in late-life schizophrenia: a longitudinal study of geriatric chronically hospitalized patients. *Biol Psychiatry* 1999; **45**: 32–40.
16. Takeda S, Yamazaki K, Miyakawa T, Takahashi H, Ikuta F, Arai H. A 64-year-old man presenting MRIs of expansive multiple high intensity areas in the cerebral white matter, cerebellum and brainstem. *Neuropathology* 2007; **27**: 403–405.
17. Wyen C, Hoffmann C, Schmeisser N *et al.* Progressive multifocal leukencephalopathy in patients on highly active antiretroviral therapy: survival and risk factors of death. *J Acquir Immune Defic Syndr* 2004; **37**: 1263–1268.

Case Report

Morel's laminar sclerosis showing apraxia of speech: Distribution of cortical lesions in an autopsy case

Zen Kobayashi,[1,2] Kuniaki Tsuchiya,[2,3] Mafuyu Takahashi,[4] Osamu Yokota,[2,5] Kazuhiro Taki,[6] Hideki Ishizu,[7] Tetsuaki Arai,[2] Haruhiko Akiyama[2] and Hidehiro Mizusawa[1]

[1]Department of Neurology and Neurological Science, Graduate School, Tokyo Medical and Dental University, Tokyo, [2]Tokyo Institute of Psychiatry, Tokyo, [3]Department of Laboratory Medicine and Pathology, Tokyo Metropolitan Matsuzawa Hospital, Tokyo, [4]Department of Neurology, Ohme Municipal General Hospital, Tokyo, [5]Department of Neuropsychiatry, Okayama University Graduate School of Medicine, Dentistry and Pharmaceutical Sciences, Okayama, [6]Department of Pathology, Musashino Redcross Hospital, Tokyo and [7]Department of Laboratory Medicine, Zikei Institute of Psychiatry, Okayama, Japan

A 57-year old man with chronic alcoholism presented with apraxia of speech and disturbance of consciousness. He had a history of gastrectomy and had been drinking alcohol. The symptoms improved with administration of thiamine, but he later developed diarrhea and delirium, and died approximately 40 days after the onset. Autopsy findings were consistent with Wernicke's encephalopathy and pellagra encephalopathy. Furthermore, laminar cortical necrosis with vacuoles and astrocytosis was found in the second and third layers of the bilateral frontal cortices, suggesting Morel's laminar sclerosis. The lesions were mainly located in the bilateral primary motor cortices. Involvement of the lower part of the left primary motor cortex may be associated with apraxia of speech in our case.

Key words: apraxia of speech, Morel's laminar sclerosis, pellagra encephalopathy, primary motor cortex, Wernicke's encephalopathy.

INTRODUCTION

A brief summary of the clinicopathological features of this case was previously reported in this journal as "Neuropathology Education" by Tsuchiya, one of the authors of this

---

paper.[1] This time, we have added the description of the clinical course, pathological findings, distribution of the cortical lesions, and review of the literature regarding Morel's laminar sclerosis, and discuss matters related to clinical practice.

The term Morel's laminar sclerosis was derived from the publication by Morel in 1939 describing unusual pathological changes in four alcoholics, taking the form of spongiform change and gliosis of the cerebral cortex, mostly confined to the third layer.[2] Although some reports described patients with Morel's laminar sclerosis,[3–6] the information regarding clinical and pathological findings has been limited.

Apraxia of speech (AOS) is caused by disturbance of motor programming of articulation, and is classically distinguished from Broca's aphasia by the preservation of the ability to write language.[7] Here, we report a patient presenting with AOS, and having histological findings indicating Morel's laminar sclerosis, as well as Wernicke's encephalopathy and pellagra encephalopathy.

CASE REPORT

The patient was a 57-year-old Japanese man, who had been living alone. After the publication of the previous paper,[1] we found that the patient had been drinking 80–100 g of alcohol per day (The duration was unclear.). Past history included diabetes mellitus, foot necrosis, angina pectoris, and gastric cancer. Because of these diseases, coronary artery bypass graft (at age 51), digital amputation (at age 55), and total gastrectomy (at age 55) were performed. Five

days before admission, his brother had contact with the patient by telephone, and the patient had been normal. On the day of admission, an acquaintance visited him and found him lying near his bed. He opened his eyes, but could not speak. On admission, body temperature was 36.0°C, blood pressure 136/115 mmHg, and heart rate 101 beats/min. General examination showed severe emaciation and surgical scars on the chest and abdomen. The palpebral conjunctiva was anemic. The second and third digits of the right foot had been amputated. On neurological examination, consciousness disturbance (easy arousal after normal calling), and hyporeflexia in the four extremities were demonstrated. He could not speak, but comprehension of spoken language was normal. Tongue protrusion was impossible. External ocular movement was normal. There was no motor paralysis in the face or limbs. Ataxia of the upper limbs was not apparent, while that of the lower limbs and trunk could not be examined. Blood test showed a white blood cell (WBC) of 7100/mm³ (normal range: 4000–9000), red blood cell (RBC) 237 × 10⁴/mm³ (normal range: 430–570 × 10⁴), platelet count (Plt) 14.9 × 10⁴/mm³ (normal range: 15–35 × 10⁴), total protein 6.3 g/dL (normal range: 6.5–8.0), urea nitrogen 41.6 mg/dL (normal range 8–20), creatinine 0.7 mg/dL (normal range: 0.6–1.2), aspartate aminotransferase (AST) 58 IU/L (normal range: < 35), alanine aminotransferase (ALT) 45 IU/L (normal range: < 40), blood sugar 180 mg/dL, and C-reactive protein 0.9 mg/dL. Brain CT demonstrated mild atrophy at the bilateral frontal and temporal lobes. Although blood thiamine was not measured, the diagnosis of Wernicke's encephalopathy was suspected based on the history of gastrectomy and drinking alcohol. Hydration with administration of thiamine was initiated, but niacin was not given. Consciousness disturbance gradually improved, but anterograde and retrograde amnesia, and time disorientation became evident. At that time, we found that his written language was normal, although the disturbance in speech output was not completely resolved. Diarrhea was also seen after the initiation of oral intake, but he was transferred to another hospital 30 days after admission. Thereafter, he developed delirium and convulsion, and was transferred back to our hospital 6 days later. He died on the same day. Artificial ventilation was not administered throughout the course. Autopsy was limited to the brain.

The brain weighed 1130 g after fixation. Macroscopically, bilateral mamillary bodies and inferior colliculi appeared gray. There were no abnormalities in the thalamus or cerebral cortex (Fig. 1). Atherosclerotic changes of the middle cerebral arteries and basilar artery were mild. Brain tissue samples were fixed post mortem with 10% formalin and embedded in paraffin. Ten-μm-thick hemispheric sections were prepared at the plane of the left frontal lobe (the most
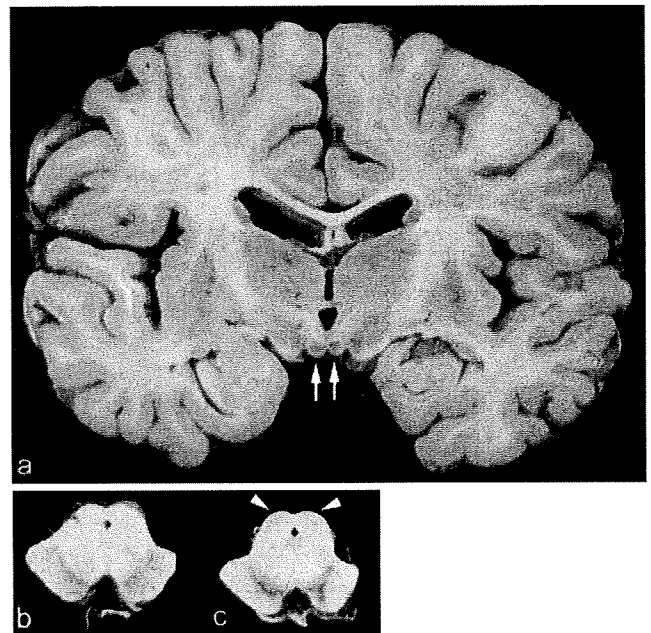
Fig. 1 (a,c) Grayish discoloration in the bilateral mamillary bodies (a, arrows) and inferior colliculi (c, arrowheads). (b) At the level of the upper midbrain. There are no macroscopic abnormalities in the periaqueductal gray matter, thalamus or cerebral cortex.

anterior section), left amygdala, bilateral mamillary bodies, left pulvinar nucleus, and right occipital lobe. The sections of upper and lower portions of the midbrain, upper and middle portions of the pons, upper, middle, and lower portions of the medulla oblongata, and bilateral cerebellum were also prepared. These sections were stained with HE, KB, Bodian, and Gallyas method, and anti-glial fibrillary acidic protein (GFAP) (rabbit, polyclonal, Dako, Glostrup, Denmark, 1:1000). Reticulin silver stain was also performed to visualize the capillaries.

Microscopic examination demonstrated necrotic foci with many vacuoles, accompanied by proliferation of macrophages and astrocytes, and capillary proliferation in the bilateral mamillary bodies and left inferior colliculi (Figs 2,3). Pinpoint hemorrhages were seen in the right mamillary body (Fig. 2c) and bilateral inferior colliculi. Neurons were relatively preserved in the lesion (Fig. 2d). Periaqueductal gray matter and oculomotor nucleus were not involved. In the thalamus, neuronal loss with astrocytosis was obvious in the bilateral mediodorsal nuclei, anterior nuclei (Fig. 3c), and left pulvinar nuclei. In the bilateral inferior olivary nucleus, patchy neuronal loss (Fig. 3d) with astrocytosis was evident. There were no abnormalities in the hypoglossal nucleus or cerebellum. These findings suggested the diagnosis of Wernicke's encephalopathy. In addition, central chromatolysis of the neurons without astrocytic or microglial changes was evident in the Betz
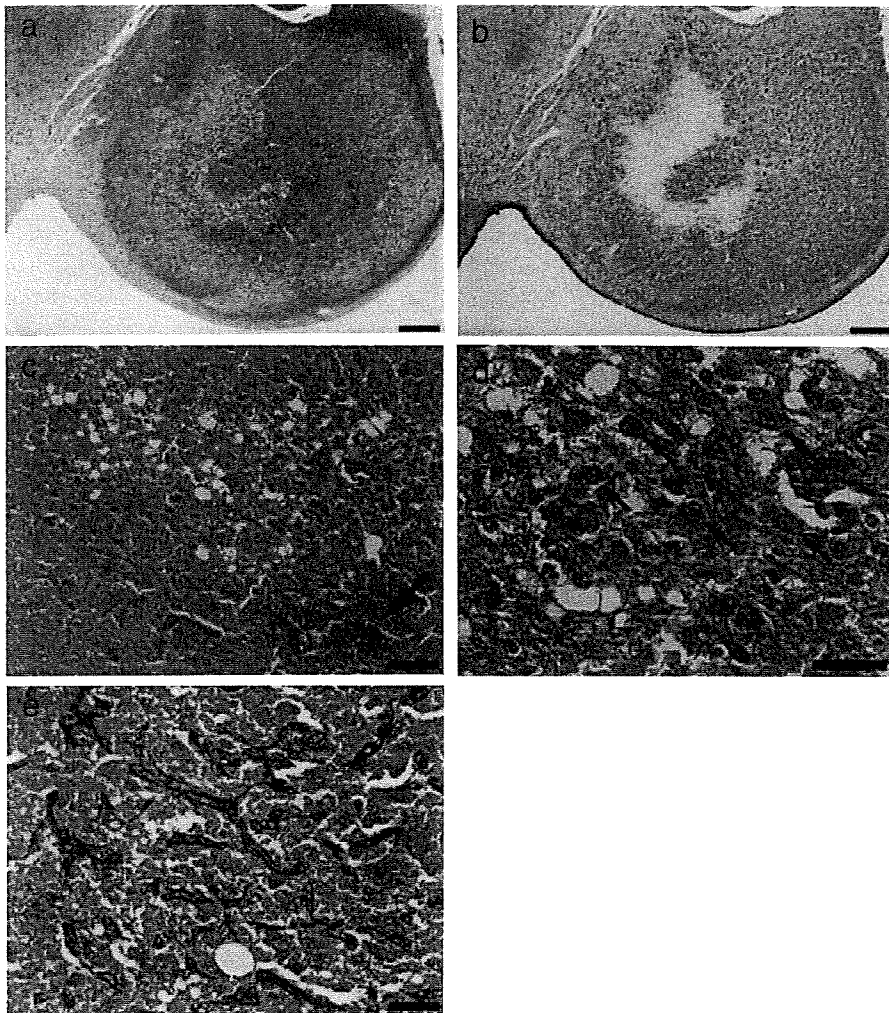
Fig. 2 (a) and (b) are serial sections. (a) Necrotic lesions in the right mamillary body. Bar = 500 μm. (b) Astrocytosis and central necrosis. Bar = 500 μm. (c) Many vacuoles and hemorrhages (arrow) in the right mamillary body. Bar = 100 μm. (d) Relative preservation of the neurons (arrows) in the right mamillary body. Bar = 50 μm. (e) Capillary proliferation in the right mamillary body. Bar = 50 μm. (a) KB stain, (b) GFAP stain, (c, d) HE stain, (e) Reticulin silver stain.

cells (Fig. 3e), pontine nucleus (Fig. 3f), left abducens nucleus, and bilateral cuneate nucleus, indicating pellagra encephalopathy. Furthermore, laminar cortical necrosis with vacuoles and astrocytosis was found in the second and third layers of the bilateral frontal cortices (Fig. 4). The vacuoles were partly seen in the first layer. The distribution of cortical lesions is shown in Figure 5. The lesions were mainly located in the bilateral primary motor cortices. On the left side, the lower part of the primary motor cortex was involved. The deep layers of the cortex were preserved. Neither thrombi nor atherosclerotic changes were observed in the vessels adjacent to the lesions. Alzheimer's type-II astrocytes were absent in the cerebral cortex and basal ganglia. There were no ischemic changes in the hippocampal pyramidal cells or cerebellar Purkinje cells. The Braak stage of neurofibrillary tangles was stage I. There were no Lewy bodies or Pick bodies. In other words, cortical changes cannot be explained by ischemia, hypoxia, hepatocerebral degeneration, or neurodegenerative diseases.

DISCUSSION

Clinically, our patient presented with AOS that improved after the administration of thiamine. He also developed diarrhea and delirium probably associated with pellagra. At autopsy, the diagnosis of Wernicke's encephalopathy and pellagra encephalopathy was confirmed. Furthermore, laminar cortical necrosis with vacuoles and astrocytosis was found in the second and third layers of the bilateral frontal cortices, suggesting Morel's laminar sclerosis.

Thiamine deficiency, which is considered a cause of Wernicke's encephalopathy, damages the mamillary bodies, medial thalamus, and periaqueductal gray matter. Other areas that are sometimes affected include the corpora quadrigemina, reticular formation of the midbrain, pontine tegmentum, superior vermis of the cerebellum,[8] and inferior olivary nucleus.[9] Observed lesions include loosening of the neuropil and vascular changes such as hemorrhage, capillary proliferation/dilatation, and endothelial swelling in the mamillary bodies and the subependymal structures

© 2009 Japanese Society of Neuropathology